CORE
Metadata, citation and similar papers at core.ac.uk
Provided by MUCC (Crossref)

Biosci. Rep. (2013) / **33** / art:e00012 / doi 10.1042/BSR20120101
Original Paper
OPEN ACCESS

Electrical hypothesis of toxicity of the Cry toxins for mosquito larvae

Victor V. LEMESHKO*[1] and Sergio ORDUZ†

*Escuela de Física Universidad Nacional de Colombia, sede Medellín, Calle 59-A, No. 63-20, Medellín, Colombia, and †Escuela de Biociencias, Facultad de Ciencias, Universidad Nacional de Colombia, sede Medellín, Calle 59-A, No. 63-20, Medellín, Colombia

Synopsis

Many electrical properties of insect larval guts have been studied, but their importance for toxicity of the Cry-type toxins has never been reported in the literature. In the present work, we observed potential-dependent permeabilization of plasma membrane by several polycationic peptides derived from the Cry11Bb protoxin. The peptide BTM-P1d, all D-type amino acid analogue of the earlier reported peptide BTM-P1, demonstrated high membrane-permeabilizing activity in experiments with isolated rat liver mitochondria, RBC (red blood cells) and mitochondria in homogenates of *Aedes aegypti* larval guts. Two larger peptides, BTM-P2 and BTM-P3, as well as the Cry11Bb protoxin treated with the protease extract of mosquito larval guts showed similar effects. Only protease-resistant BTM-P1d, in comparison with other peptides, displayed *A. aegypti* larval toxicity. Taking into account the potential-dependent mechanism of membrane permeabilization by studied fragments of the Cry11Bb protoxin and the literature data related to the distribution of membrane and transepithelial potentials in the *A. aegypti* larval midgut, we suggest an electrical hypothesis of toxicity of the Cry toxins for mosquito larvae. According to this hypothesis, the electrical field distribution is one of the factors determining the midgut region most susceptible for insertion of activated toxins into the plasma membrane to form pores. In addition, potential-dependent penetration of short active toxin fragments into the epithelial cells could induce permeabilization of mitochondria and subsequent apoptosis or necrosis.

Key words: Cry toxin, larval midgut, membrane permeabilization, mitochondrion, plasma membrane, polycationic peptide

Cite this article as: Lemeshko, V.V. and Orduz, S. (2013) Electrical hypothesis of toxicity of the Cry toxins for mosquito larvae. Biosci. Rep. **33**(1), art:e00012.doi:10.1042/BSR20120101

INTRODUCTION

Insecticidal Cry toxins are the major components of crystalline protein inclusions produced by the bacterium *Bacillus thuringiensis* during sporulation [1]. The use of proteins of this type rather than conventional chemical pesticides has been considered preferable for insect control due to their high specificity and environmental safety [2,3]. Creation of new toxin variants with higher membrane permeabilizing activity has been considered as an important biotechnological perspective [4].

The mechanism of toxicity of the Cry-type proteins for insect larvae has been attributed to their ability to permeabilize the midgut epithelial cells [1,2,5,6]. It takes place after solubilization of δ-endotoxin crystals in larval guts and subsequent partial proteolysis of the protoxins [1,7,8]. Binding to the specific membrane receptors of midgut epithelial cells has been suggested to be an important determinant for insect specificity of the δ-endotoxins [2,6,9,10], although the mechanism(s) of their toxicity for different insects is not yet clear.

Some protoxins or their fragments are also able to directly, without specific receptors, permeabilize lipid bilayers of artificial planar lipid membrane [11–16], liposomes [17–21] or the plasma membrane of RBC (red blood cells) [18,22,23]. Nevertheless, the presence of receptors in some midgut epithelial cells seems to decrease the effective concentrations of δ-endotoxins to kill insect larvae [12,13] and to increase the selectivity of their action [9,10].

Regarding the precise mechanism of permeabilization of the larval midgut epithelial cells with δ-endotoxins, the 'umbrella model' is widely recognized [4] suggesting that the helices α4 and α5 of the pore-forming domain I of *B. thuringiensis* Cry toxins insert into the membrane, while the remaining helices form the ribs of the umbrella on the membrane surface. Earlier, we

Abbreviations used: FCCP, carbonyl cyanide *p*-trifluoromethoxyphenylhydrazone; RAMF, rotenone, antimycin A, myxothiazol, FCCP; RBC, red blood cell.

[1] To whom correspondence should be addressed (email vvasilie@unal.edu.co).

© 2013 The Author(s) This is an Open Access article distributed under the terms of the Creative Commons Attribution Non-Commercial Licence (http://creativecommons.org/licenses/by-nc/2.5/) which permits unrestricted non-commercial use, distribution and reproduction in any medium, provided the original work is properly cited

have designed a new peptide, BTM-P1, composed of 26 amino acid residues [24–28] with the sequence corresponding to a significant part of the α2a helix of the Cry11Bb protoxin [29], i.e. to one of the ribs of the umbrella [4]. The peptide demonstrated high ability to permeabilize mitochondrial [24–26,28] and RBC membranes [27,28], as well as revealing high antimicrobial activity [25,26]. Taking into account these data, we have proposed the 'damaged umbrella' model, according to which the BTM-P1 fragment of the 'damaged rib' is also inserted into the membrane [27]. Interestingly, the retro-analogue of BTM-P1, retro-BTM-P1, demonstrated significantly lower membrane-permeabilizing effects [28].

The most important feature of the membrane permeabilization by the polycationic peptide BTM-P1 is its strong dependence on the membrane potential (minus inside) [24,27,28]. This allows us to assume that not only specific receptors, but also the distribution of electrical potentials in different parts of the insect midgut might be an important factor influencing the cell susceptibility to pore-forming domain I of the *B. thuringiensis* Cry toxins or even to their shorter proteolytical fragments. It is known, for example, that the electrical transepithelial potential (lumen negative) of the anterior midgut in *Aedes aegypti* larvae is the opposite to that of the posterior midgut (lumen positive) [30–33]. In addition, the most powerful generator of the plasma membrane potentials in the larval epithelial cells, the H^+ V-type proton ATPase, is distributed asymmetrically: in the basal membrane of the anterior midgut and in the apical membrane of the posterior midgut [34–37].

In the present work, we demonstrate that the polycationic peptide BTM-P1d, composed of all D-amino acids, has a membrane-permeabilizing activity similar to that of BTM-P1 (all L-type amino acid peptide) in experiments with isolated rat liver mitochondria, RBC and mitochondria in gut homogenates of *A. aegypti* larvae. The mitochondria-permeabilizing activity was also demonstrated for larger peptides, such as BTM-P2 (37 amino acid residues) and BTM-P3 (60 amino acids residues), derived from the Cry11Bb protoxin and containing BTM-P1 sequence as their part at the C-terminus, as well as for the Cry11Bb protoxin treated with the larval gut protease extract, but not for the native protoxin. Only BTM-P1d, at low concentration, in comparison with the protease-sensitive peptides BTM-P1, BTM-P2 or BTM-P3, was highly toxic for *A. aegypti* larvae. As a result, we suggest an electrical hypothesis of toxicity of the Cry toxins for mosquito larvae, which is based on the potential-dependent mechanism of membrane permeabilization by BTM-P1 [24,27,28] and by other polycationic peptides derived from the Cry11Bb protoxin, shown in this work. The hypothesis predicts that the electrical field distribution within the midgut of insect larvae is crucial for insertion of toxins and of their active proteolytic fragments into the plasma membrane to form pores. High plasma membrane potential should also favour penetration of some active peptides into the epithelial cells of certain midgut regions with subsequent permeabilization of mitochondria. This concept is supported by the literature data related to the distribution of membrane and transepithelial potentials in the anterior and posterior midguts of *A. aegypti* larvae [30–33,38–40].

MATERIAL AND METHODS

Materials

The polycationic peptides were designed in our laboratory on the basis of the natural sequence of the Cry11Bb protoxin and were synthesized by GenScript Corporation. The peptides composed of all L-amino acids were the following: BTM-P1 of 95.4% purity with the sequence of VAPIAKYLATALAKWALKQGFAKLKS, BTM-P2 of 94.2% purity with the sequence of IEPSIAPALIAVAPIAKYLATALAKWALKQGFAKLKS and BTM-P3 of 92.4% purity with the sequence of MENNSFNVLANNNMSSFPLFNSKIEPSIAPALIAVAPIAKYLATALAKWALKQGFAKLKS. The peptide BTM-P1d of 94.1% purity was composed of all D-amino acids with the sequence of vapiakylatalakwalkqgfaklks. The chemicals were purchased from Sigma Chemical Co. and valinomycin from Merck.

Evaluation of *A. aegypti* larval viability

The *A. aegypti* colony was maintained on artificial diet at 30 °C, 70–80% relative humidity and 12:12 h light:dark photoperiod. Ten of each 1st, 2nd or 3rd instar larvae were placed in 24-well plates containing 1 ml of dechlorinated tap water. The peptides dissolved in 100 mM HEPES–Tris buffer, pH 7,4, with 10% (v/v) DMSO were added to a final concentration of 5 and 10 μM. Each treatment was performed with five replicates. Larval survival was scored every hour until the 9th h and at 24 h after the treatment. Buffer, at volumes 5 or 10 μl, was added to the control groups.

Preparation of homogenates of *A. aegypti* larval guts

Guts excised from early 4th instar *A. aegypti* larvae (200 in 0.5 ml of medium containing 100 mM sucrose, 75 mM KCl, 10 mM inorganic phosphate, 1 mM EGTA, 5 mM HEPES–KOH, pH 7.2) were homogenized in a Polytron homogenizer at 30 000 rev./min at 0–4 C°.

Preparation of Cry11Bb protoxin and of its hydrolysate in the natural protease extract of *A. aegypti* larval guts

The Cry11Bb protoxin was obtained from the acrystalliferous recombinant strain SPL-407 of *B. thuringiensis* subsp. *thuringiensis*. It had been transformed with the plasmid pSOB containing DNA insert encoding the protoxin [41]. The recombinant cells were grown in M1 medium [42] supplemented with 25 μg/ml erythromycin for 72 h at 30 °C and sedimented by centrifugation. To solubilize the crystals, the pellet was treated with 50 mM 3-(cyclohexylamino)-propane sulfonate, pH 10.6, containing 0.05% 2-mercaptoethanol. The insoluble material was removed by centrifugation. Concentration of the obtained soluble toxin was 21 mg/ml determined by the method of Bradford [43], using BSA as standard.

© 2013 The Author(s) This is an Open Access article distributed under the terms of the Creative Commons Attribution Non-Commercial Licence (http://creativecommons.org/licenses/by-nc/2.5/) which permits unrestricted non-commercial use, distribution and reproduction in any medium, provided the original work is properly cited

The mosquito larval protease extract was prepared from the guts excised from early 4th instar *A. aegypti* larvae as described in [44]. The soluble Cry11Bb protoxin was hydrolysed for 2 h at 37 °C with this protease extract at an extract:toxin ratio of 1:50 (w/w protein) that resulted in production of two major fragments of approximately 30 and 35 kDa, as has been shown earlier [44]. The possibility of formation of shorter fragments, down to peptides, under such treatment has not been studied.

Isolation of rat liver mitochondria

Mitochondria from liver of male Sprague–Dawley rats (starved overnight) were isolated by the method of differential centrifugation as described earlier [45], following the principles outlined in the Guide for the Care and Use of Laboratory Animals published by the USA National Institutes of Health (NIH Publication No. 85-23, revised 1996) and approved by the Local Ethics Committee of the National University of Colombia, Medellin Branch. Previously cooled liver was homogenized in medium containing 210 mM mannitol, 70 mM sucrose, 2.5 mM $MgCl_2$, 1 mM EGTA–KOH, 0.3 mg/ml BSA (fatty acid-free fraction V), 10 mM HEPES–KOH, pH 7.2, at 0–4 °C. The first mitochondrial pellet was resuspended in the medium containing 210 mM mannitol, 70 mM sucrose, 50 μM EGTA–KOH, 0.3 mg/ml BSA and 10 mM Hepes–KOH, pH 7.2, and mitochondria were sedimented again. This procedure of mitochondria washing was repeated and finally mitochondria were resuspended in 1 ml of the same medium, but without BSA.

Isolation of RBC from white rats

RBC were isolated as described in [46] with slight modifications. Approximately 5 ml of rat blood were mixed with 20 ml of the medium composed of 120 mM NaCl, 10 mM EDTA, 5 mM sodium citrate and 5 mM Tris/HCl, pH 7.4, and centrifuged at 600 ***g*** for 10 min (Jouan centrifuge RM1812). The pellet was washed three times by gentle resuspension of the cells in 20 ml of 150 mM NaCl, 5 mM Tris/HCl, pH 7.4, and subsequent centrifugation at 600 ***g*** for 10 min. The final pellet was resuspended in the same medium supplemented with 10 mM glucose to the final haematocrit of 20 %.

Monitoring of the inner membrane potential of mitochondria

The inner membrane potential of rat liver mitochondria was monitored with the potential-sensitive fluorescent probe safranin O (520 nm excitation, 580 nm fluorescence) as described in [47] using the Aminco-Bowman Series 2 spectrofluorimeter. Mitochondria, at the concentration of 0.5 mg protein/ml, were added to the incubation medium KNPE composed of 150 mM KNO_3, 5 mM inorganic phosphate, 20 μM EGTA, pH 7.2, supplemented with 2.5 mM succinate and 10 μM safranin O.

Monitoring of the redox state of mitochondrial pyridine nucleotides

The level of reduced forms of endogenous pyridine nucleotides, NAD(P)H, in isolated rat liver mitochondria and in larval midgut homogenates was monitored by fluorescence at 450 nm using the Aminco-Bowman Series 2 Luminescence Spectrometer. With the aim to minimize the influence of turbidity of the suspension on fluorescence measurements and to decrease the effect of the internal filter, the exciting and emitting light beams were focused on the 1.5×1.5 mm corner of the cuvette as described in [48], and the excitation wavelength of 365 nm was selected instead of 340 nm. Mitochondria, at final concentration of 0.5 mg protein/ml, or larval midgut homogenates at the equivalent of 12 larval guts/ml, were added to the incubation medium composed of 100 mM sucrose, 75 mM KCl, 10 mM potassium phosphate, 50 μM EGTA, 5 mM HEPES, pH 7.2 (the SKPH medium). The drop of the inner membrane potential, as a result of mitochondria permeabilization, was revealed by a decrease of the NAD(P)H fluorescence due to an accelerated oxidation of pyridine nucleotides.

Evaluation of the outer membrane permeability of mitochondria to cytochrome *c*

Rat liver mitochondria, 0.5 mg protein/ml, were incubated in isotonic medium composed of 100 mM sucrose, 75 mM KCl, 20 μM EGTA, 5 mM potassium phosphate, 5 mM HEPES–KOH, pH 7.2, supplemented with 2.5 mM succinate. After 1 min of mitochondria preincubation, 0.7 μM BTM-P1 was added and subsequent oxidation of endogenous NAD(P)H was observed. After approximately 3 min, the respiratory chain inhibitors (2.5 μM rotenone, 0.5 μM antimycin A, 0.5 μM myxothiazol) and 1 μM protonophoric uncoupler FCCP (carbonyl cyanide *p*-trifluoromethoxyphenylhydrazone) (RAMF) were added followed by the addition of 20 μM NADH. Under these conditions, the rate of oxidation of added NADH was limited by the outer membrane permeability to endogenous cytochrome *c*, as shown earlier [49].

Monitoring of the plasma membrane potential of RBC

The plasma membrane potential of RBC was monitored by the potential-sensitive fluorescent probe $DiSC_3(5)$ [50]. Two types of incubation media were used: (i) NaCl medium composed of 150 mM NaCl, 0.1 mM KCl, 5 mM HEPES–NaOH, pH 7.2 and (ii) the NaCl–sucrose medium composed of 63 mM NaCl, 125 mM sucrose, 0.1 mM KCl, 5 mM HEPES–NaOH, pH 7.2. RBC were added at the final haematocrit of 0.2 %. Both media were supplemented with $DiSC_3(5)$ at the final concentration of 2 μM. Potential-dependent capture of the cationic probe $DiSC_3(5)$ by RBC led to a decrease of its fluorescence intensity (648 nm excitation, 668 nm fluorescence). Valinomycin was added to the RBC suspension to the final concentration of 1 μM in order to artificially generate a relatively high membrane potential.

© 2013 The Author(s) This is an Open Access article distributed under the terms of the Creative Commons Attribution Non-Commercial Licence (http://creativecommons.org/licenses/by-nc/2.5/) which permits unrestricted non-commercial use, distribution and reproduction in any medium, provided the original work is properly cited

The peptides were added to the suspension of normal RBC, or of RBC pre-incubated with valinomycin.

Observation of mitochondrial swelling and of shrinkage-swelling of RBC

Mitochondrial swelling was monitored simultaneously with the NAD(P)H or safranin O fluorescence using a modified cuvette holder [48] for the Aminco-Bowman Series 2 spectrofluorimeter. One of the two auxiliary channels of this equipment allows measurement of 90°-dispersion of light emitted by an infra red light-emitting diode (920 nm). The dispersed light was detected by the additionally mounted photodiode and amplifier before it was registered in an auxiliary channel [48]. In the same manner, an increase or decrease in light dispersion in the RBC suspension was monitored allowing observation of cell shrinkage or swelling, respectively, as was shown previously [28]. Light dispersion of RBC was monitored simultaneously with $DiSC_3(5)$ fluorescence described above.

The samples were constantly stirred with the magnetic stirrer and maintained at the temperature of 30 °C. The data are presented as a means ± S.E.M.

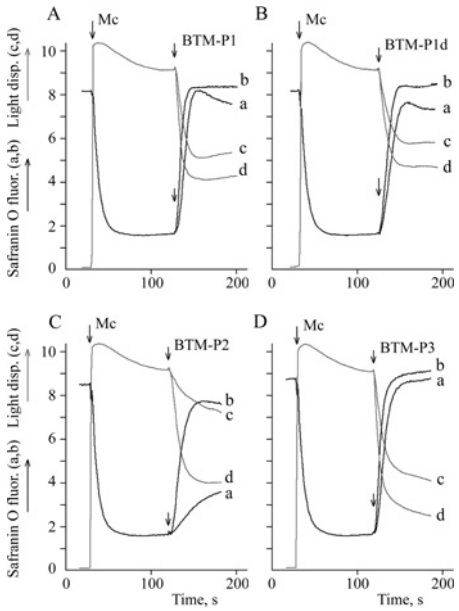

Figure 1 Influence of the peptides derived from the Cry11Bb protoxin on the inner membrane potential of rat liver mitochondria monitored by safranin O fluorescence (a,b), and on mitochondrial swelling monitored by light dispersion (c,d)

Mitochondria (0.5 mg/ml protein) were added to the KNPE medium supplemented with 2.5 mM succinate and 10 μM safranin O; (a,c) 0.5 μM peptide; (b,d) 1.0 μM peptide.

RESULTS

Earlier, we have designed the polycationic peptide BTM-P1 with very high membrane permeabilizing activity [24,27,28]. This peptide contains four hydrophobic amino acid residues at the N-terminus and a fragment of 22 amino acid residues [24,26,27] that belongs to the α2 helix of domain I of the *B. thuringiensis* Cry11Bb protoxin [29].

In the present study, we also designed an all D-type amino acid analogue of BTM-P1, the proteolysis-resistant peptide BTM-P1d and two larger all L-type amino acid peptides, BTM-P2 and BTM-P3, which include BTM-P1 as their C-terminus fragment. Both of the larger peptides were derived from the Cry11Bb protoxin sequence. To evaluate the membrane permeabilizing activities of these new peptides, we first studied their influence on the inner membrane potential (Figure 1; curves a,b) and swelling of rat liver mitochondria (Figure 1; curves c,d) at the peptide concentrations of 0.5 μM (Figure 1; curves a,c) and 1.0 μM (Figure 1; curves b,d). According to the obtained data, very similar inner membrane potential decrease and mitochondrial swelling were caused by peptides BTM-P1 (Figure 1A) and BTM-P1d (Figure 1B), with slightly higher activity for BTM-P1. The larger peptides, BTM-P2 (Figure 1C) and BTM-P3 (Figure 1D), demonstrated effects comparable with those of BTM-P1 (Figure 1A). At the concentration of 0.5 μM, the intermediate size peptide BTM-P2 showed the lowest activity (Figure 1C; curves a,c).

The cationic probe safranin O, used in these experiments to monitor the membrane potential (Figure 1), has been found to decrease the efficiency of some polycationic peptides to permeabilize mitochondria [51]. That is why the inner membrane potential was also monitored indirectly, by measuring fluorescence intensity of mitochondrial endogenous NAD(P)H (Figure 2). The highly reduced state of pyridine nucleotides of mitochondria, energized under succinate oxidation (Figure 2), was maintained due to the energy-dependent RET (reverse electron transport) through complex I of the respiratory chain and after that, through the proton-translocating energy-dependent THG (transhydrogenase) of the inner membrane, as shown in Figure 3(A). It means that the steady-state level of mitochondrial pyridine nucleotides depends on the inner membrane proton electrochemical gradient composed of the membrane electrical potential and delta pH. The peptides BTM-P1 and BTM-P1d at 0.2 μM concentration caused a rapid decrease in the intensity of NAD(P)H fluorescence (Figure 2A; curves a,c) that was accompanied by a fast decrease in light dispersion of the mitochondrial suspension (Figure 2A; curves b,d). Slightly lower activities were observed for peptides BTM-P2 (Figure 2B) and BTM-P3 (Figure 2C).

In contrast to the peptides BTM-P1, BTM-P2 and BTM-P3, derived from the Cry11Bb protoxin, the soluble native protoxin (C) did not cause any decrease in the mitochondrial NAD(P)H fluorescence (Figure 2D; curve a) and did not induce swelling of rat liver mitochondria (Figure 2D; curve b). To evaluate, whether the natural hydrolysis of this protoxin by larval gut proteases could generate fragments capable of mitochondria permeabilization, the soluble Cry11Bb protoxin was treated with the protease extract of *A. aegypti* larval gut. The hydrolysed Cry11Bb

© 2013 The Author(s) This is an Open Access article distributed under the terms of the Creative Commons Attribution Non-Commercial Licence (http://creativecommons.org/licenses/by-nc/2.5/) which permits unrestricted non-commercial use, distribution and reproduction in any medium, provided the original work is properly cited

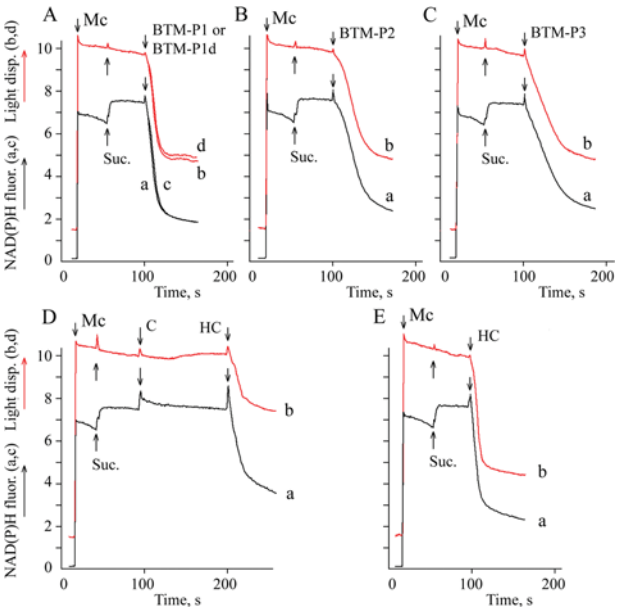

Figure 2 Influence of the peptides derived from the Cry11Bb protoxin and of the solubilized (C) and hydrolysed (HC) Cry11Bb protoxin on the NAD(P)H fluorescence of rat liver mitochondria (a,c) and on mitochondrial swelling monitored by light dispersion (b,d)

Mc – mitochondria (0.5 mg/ml protein) added to SKPH medium. Suc., 2.5 mM succinate; C, 57 μg/ml of the solubilized Cry11Bb; HC, 57 μg/ml of the Cry11Bb hydrolysed in the larval midgut extract; the final peptide concentration was 0.2 μM.

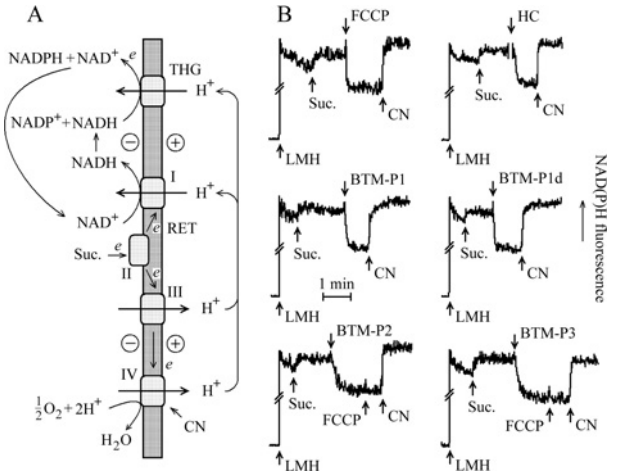

Figure 3 The energy-dependent RET maintains the reduced state of mitochondrial pyridine nucleotides (A) and the steady-state level of NAD(P)H fluorescence of larval midgut homogenate (LMH; B) affected by protonophoric uncoupler FCCP, by the natural hydrolysate of the Cry11Bb protoxin (HC) and by the peptides derived from the Cry11Bb protoxin

The LMH, in the equivalent of 12 guts, was added to 1 ml SKPH medium. Energy-dependent THG; I, II, III, IV, respiratory chain complexes. Suc., 2.5 mM succinate; FCCP, 1 μM FCCP; CN, 0.5 mM KCN; HC, 57 μg/ml of Cry11Bb hydrolysed in the larval gut extract. The final peptide concentration was 1 μM.

protoxin (HC), added after the untreated soluble protoxin (C), caused a marked decrease in the steady-state level of mitochondrial NAD(P)H (Figure 2D; curve a) and induced mitochondrial swelling (Figure 2D; curve b). Even more pronounced effects, similar to those caused by the studied peptides (Figures 2A–2C) were observed when the hydrolysed Cry 11Bb protoxin (HC) was added to the mitochondrial suspension in the absence of native protoxin (Figure 2E).

The intensity of NAD(P)H fluorescence of larval gut homogenates was also increased after the addition of succinate (Figure 3B), presumably due to the energy-dependent RET mentioned above (Figure 3A). This fluorescence intensity was sensitive to protonophoric uncoupler FCCP (Figure 3B), which is known to dissipate proton electrochemical gradient of the inner membrane of mitochondria. After that, the addition of KCN, known to inhibit the respiratory chain at the level of cytochrome a_3, allowed fluorescence intensity recovery (Figure 3B), as a result of reduction of mitochondrial pyridine nucleotides by endogenous substrates.

The effects similar to that caused by FCCP in larval midgut homogenates (Figure 3B) were also observed after the addition of the natural hydrolysate of Cry11Bb (HC), as well as after the addition of 1 μM BTM-P1 or BTM-P1d (Figure 3B). A similar decrease in the blue fluorescence, although slower, was also caused by peptides BTM-P2 or BTM-P3 (Figure 3B). In all these cases, the addition of KCN caused fluorescence recovery.

BTM-P1 influence on the rate of oxidation of external NADH in rat liver mitochondria was studied (Figure 4) to evaluate its ability to permeabilize the mitochondrial outer membrane. The oxidation of external NADH is known to depend on cytochrome *c* shuttling between the outer surface of damaged or permeabilized outer membrane (cytochrome b_5) and the cytochrome-*c* oxidase of the inner membrane (see [49] and references therein). As shown, 1 μM BTM-P1 increased the oxidation of external NADH by more than one order of magnitude (Figure 4). It indicates that BTM-P1 is capable of promoting cytochrome *c* release from mitochondria. Epithelial cells of *A. aegypti* larvae are rich in mitochondria to provide the energy necessary for transepithelial ion transport [34,52]; therefore they might be very susceptible to peptides such as BTM-P1.

The ability of the peptides to permeabilize plasma membrane was evaluated using RBC with normally low membrane potential (Figures 5A and 5C) and RBC with a high membrane potential generated in the presence of valinomycin (Figures 5B and 5D). The peptides BTM-P1 (Figure 5A; curves a,b), BTM-P1d (Figure 5A; curves c,d) and BTM-P2 (Figure 5C; curves c,d) at concentrations up to 5 μM did not essentially change the plasma membrane potential monitored by the potential-sensitive fluorescent probe DiSC3(5) (curves a,c) and did not affect light dispersion (curves b,d) in the suspension of normal cells (Figures 5A and 5C). Small decrease in RBC light dispersion was observed in the presence of 2,5 μM BTM-P3, although its effect on the membrane potential was negligible (Figure 5C; curves a,b). In the presence of valinomycin (Figures 5B and 5D), these peptides caused a drop of the initially high plasma membrane potential

© 2013 The Author(s) This is an Open Access article distributed under the terms of the Creative Commons Attribution Non-Commercial Licence (http://creativecommons.org/licenses/by-nc/2.5/) which permits unrestricted non-commercial use, distribution and reproduction in any medium, provided the original work is properly cited

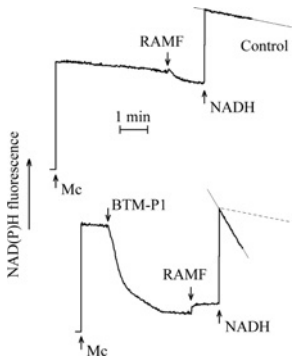

Figure 4 BTM-P1 increases the outer membrane permeability of rat liver mitochondria to cytochrome *c*, according to a strong activation of the external pathway of NADH oxidation
Rat liver mitochondria, 0.5 mg protein/ml, were incubated in the isotonic medium composed of 100 mM sucrose, 75 mM KCl, 20 μM EGTA, 5 mM potassium phosphate, 5 mM HEPES-KOH, pH 7.2, 2.5 mM succinate. BTM-P1, 0.7 μM BTM-P1; RAMF, 2.5 μM rotenone, 0.5 μM antimycin A, 0.5 μM myxothiazol; and 1 μM FCCP; NADH, 20 μM.

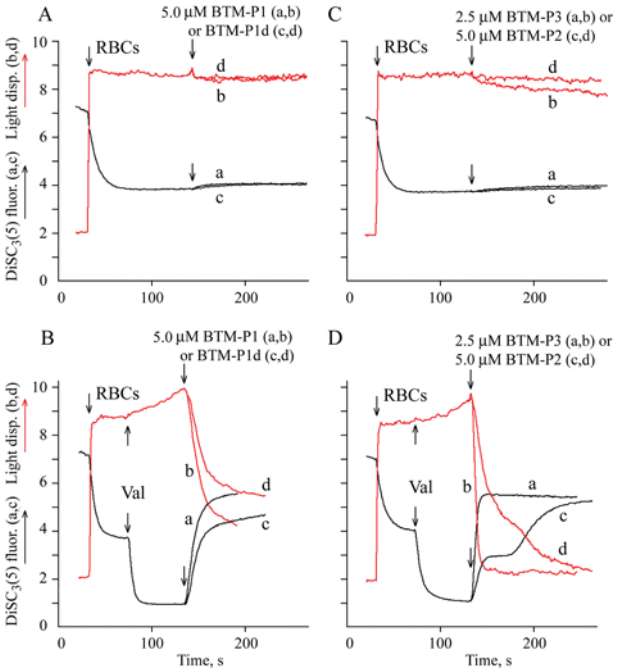

Figure 5 Influence of the peptides derived from the Cry11Bb protoxin on DiSC3(5) fluorescence (a,c) and on light dispersion (b,d) in the suspension of RBC with normal (A,C) and artificially generated high membrane potential (B,D)
RBC (0.2% haematocrit) were added to the incubation medium composed of 150 mM NaCl, 0.1 mM KCl, 5 mM Tris/HCl, pH 7.4 and 2 μM DisC3(5). Val, 1 μM valinomycin.

(Figures 5B and 5D; curves a,c) and induced a fast decrease in light dispersion (Figure 5B and 5D; curves b,d). The largest peptide, BTM-P3, showed the most significant effect even at lower peptide concentration (Figure 5D; curves a,b). In these experiments, the effect of BTM-P1 (Figure 5B; curves a,b) was slightly higher than that of BTM-P1d (Figure 5B; curves c,d).

The biphasic response of light dispersion in the suspension of RBC (preincubated with valinomycin) was observed after the addition of 1 μM BTM-P1 (Figure 6A; curve b) or 1 μM BTM-P1d (Figure 6B; curve b) when NaCl-sucrose medium (Figure 6) was used instead of NaCl medium (Figure 5). The drop of the initially high membrane potential (Figures 6A and 6B; traces a) after the addition of the peptides coincided with the first phase of light dispersion changes, i.e. with the cell shrinkage phase of the biphasic response (Figures 6A and 6B; curve b). This is clear from a comparison of the positive peaks of the corresponding first derivates (c and d, respectively, in Figures 6A and 6B). The negative peaks of the first derivatives (Figures 6A and 6B; curve d) indicate that the second phase corresponds to a high amplitude swelling (Figures 6A and 6B; curve b) of the depolarized cells (Figures 6A and 6B; a). High degree of membrane permeabilization was observed after the addition of BTM-P2 (Figure 6C; curves a,b) or BTM-P3 (Figure 6D; curves a,b) at the same 1 μM peptide concentration. No biphasic response was detected in both of these cases, in contrast to the peptides BTM-P1 and BTM-P1d, even at smaller peptide concentrations: at 0.5 μM BTM-P2 (Figure 6C; curves e,f), or at 0.25 μM BTM-P3 (Figure 6D; curves g,h).

Next, we evaluated the peptide toxicity for *A. aegypti* larvae (Figure 7), taking into account the ability of studied peptides to permeabilize isolated rat liver mitochondria (Figures 1 and 2) and to decrease the blue fluorescence intensity of larval gut homogenates (Figure 3B), related to permeabilization of gut mitochondria, as well as the potential-dependent permeabilization of the plasma membrane (Figures 5 and 6). A very slight mortality was observed for 1st instar larvae in the presence of 10 μM BTM-P1, and no toxicity was detected for 2nd and 3rd instar larvae (Figure 7). Peptides BTM-P2 and BTM-P3 had no measurable effect on the larval survival at the same experimental conditions (results not shown). On the other hand, 90% of 1st instar larvae were dead in 24 h even at 5 μM concentration of BTM-P1d. Significantly higher toxicity was observed at 10 μM BTM-P1d for all studied larval instars (Figure 7). The obtained data also showed a statistically significant increase in the larval resistance to the peptide BTM-P1d from 1st to 3rd instar larvae (Figure 7).

DISCUSSION

The electrical properties of *A. aegypti* larval gut have been studied by various scientific groups, focusing on the mechanisms of generation of specific pH values in various gut regions, on pH-dependent solubilization of protoxin crystals and amino acid absorption, but not on toxicity of the Cry toxins. The values of the membrane and transepithelial potentials of larval midgut varied in a broad range, as summarized in Figure 8. The opposite signs of transepithelial potentials in the anterior and posterior midguts are the result of the asymmetric location of the H^+ V-ATPases

© 2013 The Author(s) This is an Open Access article distributed under the terms of the Creative Commons Attribution Non-Commercial Licence (http://creativecommons.org/licenses/by-nc/2.5/) which permits unrestricted non-commercial use, distribution and reproduction in any medium, provided the original work is properly cited

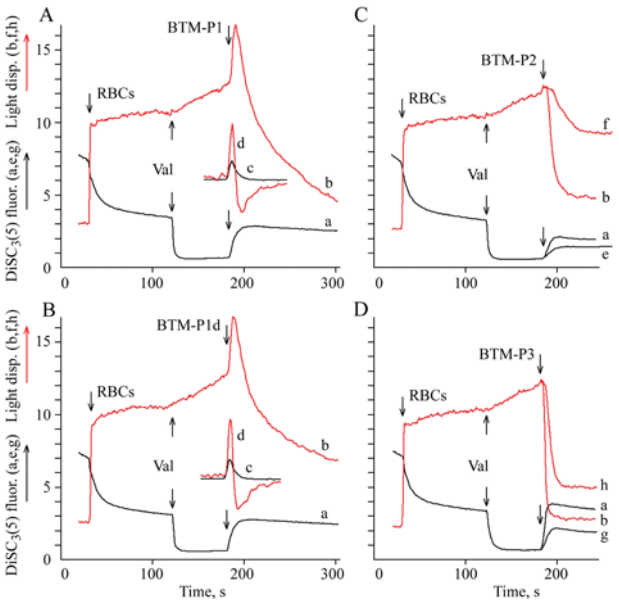

Figure 6 Influence of the peptides derived from the Cry11Bb protoxin on DiSC3(5) fluorescence (a,e,g) and on light dispersion (b,f,h) in the suspension of RBC with artificially generated high membrane potential in relatively low ionic strength medium

RBC (0.2% haematocrit) were added to isotonic NaCl-sucrose medium composed of 63 mM NaCl, 125 mM sucrose, 0.1 mM KCl, 5 mM Tris/HCl, pH 7.4, and 2 μM DisC3(5); Val, 1 μM valinomycin; (c,d) first derivatives of the curves a and b, respectively. The final peptide concentrations were 1 μM (a,b,c,d), 0.5 μM (e,f) and 0.25 μM (g,h).

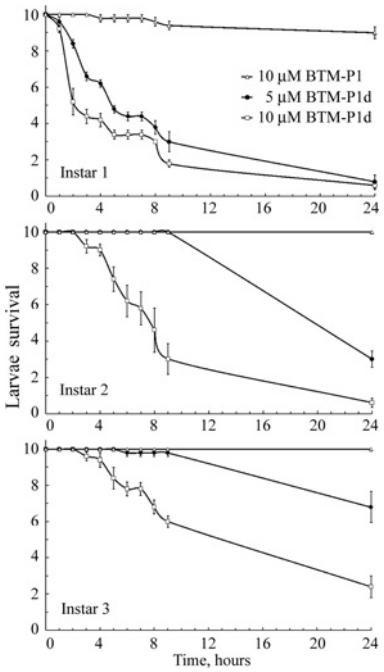

Figure 7 Survival of *A. aegypti* larvae (instars 1, 2 and 3) treated with peptides BTM-P1 and BTM-P1d

[34–37,53]: in the basal membrane of the anterior midgut and in the apical membrane of the posterior midgut. The H^+ V-ATPases are powerful generators of proton electrochemical gradients, which provide ion cycling through the midgut epithelium and alkalinization of the anterior midgut of *A. aegypti* larvae [32,33,54,55].

An equivalent electrical circuit for the anterior midgut epithelium shown in Figure 8 is significantly simplified, because two electrically distinct cell types have been reported [38]. Nevertheless, the circuit allows demonstration that a high electrical potential generated by the H^+ V-ATPase of the basal cell membrane of the anterior midgut (V_{ba}), is applied to the junction contacts (V_{ta} on the resistance R_{ta}) and to the apical membrane (V_{aa} on the resistance R_{am}), according to the Ohm's law.

High value of the luminal pH in the anterior midgut (Figure 9A), up to 11 or higher, is maintained due to the functioning of the apical membrane $2H^+/Na^+$ (or $2H^+/K^+$) antiporter [54,56,57] in combination with $nHCO_3^-/Na^+$ and CO_3^{2-}/Na^+ simporters [31,32]. The electrogenic character of these transporters allows the maintenance of a low value of the apical membrane potential V_{aa}. The cytoplasmic CO_2 (Figure 9A) is particularly generated by the mitochondrial metabolism [31]. The concentration of sodium ions in the cytoplasm is recovered by the basal Na^+/H^+ antiporter [58] and by the apical Na^+/K^+ P-ATPase that has been reported for the anterior midgut of *A. aegypti* larvae [36] (results not shown in Figure 9A for simplicity). This apical Na^+/K^+ P-ATPase would also provide additional counter ions (Na^+) for HCO_3^- and CO_3^{2-} flowing into the lumen for its alkalinization [54].

In the posterior midgut, the H^+ V-ATPase of the apical membrane generates high proton electrochemical gradient with relatively low difference of pH across the membrane due to the functioning of the ΔpH-dependent electrogenic $2H^+/Na^+$ antiporter (Figure 9A). This ion transport allows maintenance of the luminal pH<8 and of relatively high value of the apical membrane potential (V_{ap}) [53–55,59]. The voltage V_{ap} is applied to the junction contacts (V_{tp} on the resistance R_{tp}, Figure 8) and to the basal membrane (V_{bp} on the resistance R_{bm}, Figure 8), and it is a driving force for the transport of amino acids (aa) into the epithelial cells through the Na^+/aa simporter [60] (Figure 9A). The subsequent transport of amino acids through the basal membrane of the posterior midgut into the haemolymph is realized by the K^+/aa simporter [33,37,54,61] (Figure 9A) using the energy of potassium gradient generated by the basal Na^+/K^+ P-ATPase [36,62], which in addition provides transepithelial sodium cycling (Figure 9A). The functioning of the Na^+/H^+ non-electrogenic antiporter in the basal membrane [58] and of a possible anion channel permeable to HCO_3^- [33], should lead to activation of the basal Na^+/K^+ P-ATPase. A decrease in the basal membrane potential V_{bp} due to the presence of an anion channel would provide an increase in the transepithelial potential V_{tp} (Figure 9A),

The Cl^- flow through the junction contacts [31,33], which are more permeable for anions than for cations [63,64], would activate the cycling of Na^+ counter-ions through the epithelium and along the midgut and haemolymph [60] (Figure 9A).

© 2013 The Author(s) This is an Open Access article distributed under the terms of the Creative Commons Attribution Non-Commercial Licence (http://creativecommons.org/licenses/by-nc/2.5/) which permits unrestricted non-commercial use, distribution and reproduction in any medium, provided the original work is properly cited

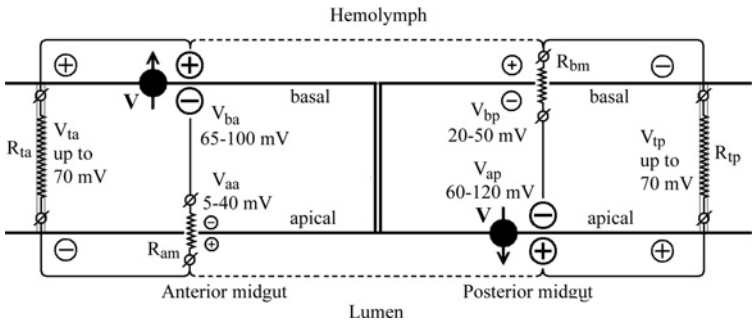

Figure 8 **Simplified schematic representation of the distribution of membrane and transepithelial potentials in the midgut of *A. aegypti* larvae**

H^+ V-ATPases, as the most powerful generators of membrane potentials in the epithelial cells, are asymmetrically located in the anterior and posterior midguts (see details in the Discussion section).

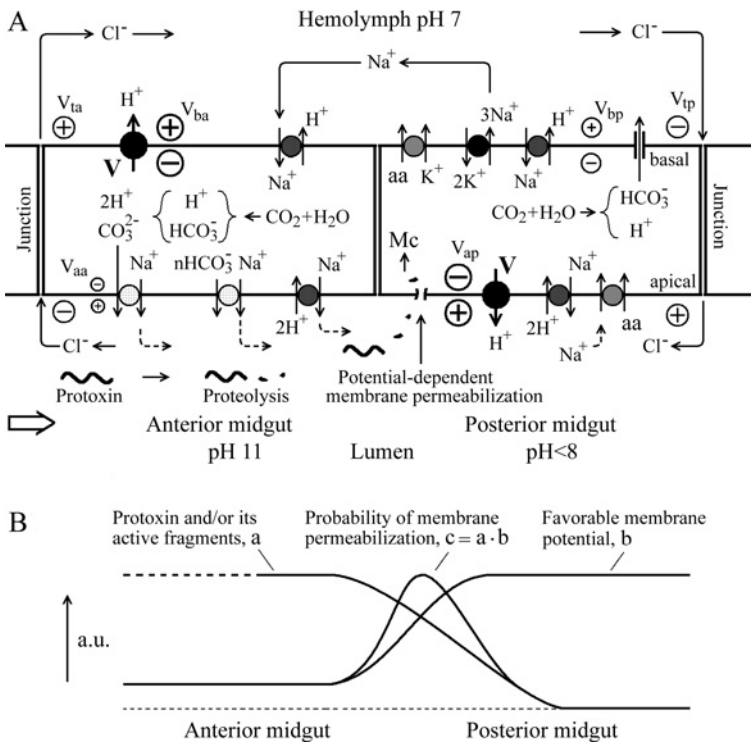

Figure 9 **Minimal electrical model of toxicity of the Cry toxins for *A. aegypti* larvae with strongly alkaline anterior midgut having the transepithelial potential opposite to that of the posterior midgut (see details in the Discussion section)**

(**A**) The distribution of some ion transporting systems providing ion cycling through the anterior and posterior midguts and allowing the maintenance of alkaline pH in the anterior midgut. Membrane-active fragments of a Cry toxin appear as a result of its initial hydrolysis and subsequently disappear due to further hydrolysis, arriving to the posterior midgut with some probability, where they can permeabilize the apical plasma membrane in a potential-dependent manner or penetrate into the cells causing mitochondria (Mc) permeabilization. (**B**) Schematic presentation of probability of the plasma membrane permeabilization by Cry protoxins and/or by their active fragments, depending on the distribution of their effective concentrations along the lumen and on the favourable membrane potential to insert them into the membrane.

Relatively low value of V_{aa} in the anterior midgut and high value of V_{ap} in the posterior midgut (Figure 8) might determine the most sensitive regions of the midgut epithelium for the membrane permeabilization by the Cry toxins and by their membrane-active fragments. It means that if some active fragments of the Cry protoxins appear in the midgut lumen as a result of proteolysis, the electrical fields might affect the insertion of such fragments into the plasma membrane of the epithelial cells (Figure 9A). If these fragments, like the studied potential-dependent peptides, have access to the cytoplasm, they might permeabilize mitochondria

© 2013 The Author(s) This is an Open Access article distributed under the terms of the Creative Commons Attribution Non-Commercial Licence (http://creativecommons.org/licenses/by-nc/2.5/) which permits unrestricted non-commercial use, distribution and reproduction in any medium, provided the original work is properly cited

(Mc) (Figure 9A) leading to subsequent release of cytochrome *c* into the cytoplasm and apoptosis. A similar effect has been described for some anticancer polycationic peptides ([65] and references therein). The presence of apoptotic cells in the insect epithelium treated with some Cry toxins has been recently reported in the literature [66]. Mitochondria-mediated induction of apoptosis by short peptides, originating from proteolysis of Cry toxins, might represent a signalling mechanism of cell death (see [67] for review), before a significant effect of pore formation in the plasma membrane takes place.

As shown in this work, various peptides, BTM-P1, BTM-P2 and BTM-P3, derived from domain I of the Cry11Bb protoxin, decreased the inner membrane potential and induced mitochondrial swelling (Figure 1). These peptides also affected the level of mitochondrial NAD(P)H (Figure 2) that strongly depends on the inner membrane potential, as explained in Figure 3A. The obtained results demonstrated that not only the studied peptides, but also the natural hydrolysate of Cry11Bb protoxin cause a strong decrease in NAD(P)H fluorescence of rat liver mitochondria (Figure 2) and in the blue fluorescence of mitochondria in larval midgut homogenates (Figure 3B). The native non-hydrolysed protoxin did not show any permeabilizing effect (Figure 2D).

Significant permeabilization of the outer membrane to cytochrome *c* by BTM-P1 was also detected, according to a strong activation of the external pathway of NADH oxidation in rat liver mitochondria (Figure 4). Similar results were obtained for other studied peptides (results not shown). In this sense, the high density of mitochondria in the posterior midgut in comparison to the anterior midgut of *A. aegypti* larvae, reported in [52], allows one to predict a higher susceptibility of the posterior midgut to the damaging action of peptides such as BTM-P1.

To damage mitochondria in the epithelial cells, the peptides should penetrate the plasma membrane. Earlier, we have shown that the permeabilization of RBC plasma membrane by BTM-P1 strongly depends on the membrane potential [24,27,28]. In the present work, we observed that the peptide BTM-P1d, similarly to BTM-P1, caused permeabilization of the RBC with artificially generated high membrane potential (− 85 mV approximately [28]), whereas it did not permeabilize normal cells with a very low membrane potential (− 10 mV approximately, see [28] for references) (Figures 5A and 5B). In addition, a strong dependence of the plasma membrane permeabilization on membrane potential was observed for larger peptides, BTM-P2 and BTM-P3 (Figure 5C and 5D). In the NaCl-sucrose medium, with a decreased ionic strength that might be similar to that of the lumen of larvae incubated in fresh water, all studied peptides demonstrated significantly stronger effects than observed in the NaCl medium (compare the respective 1 μM peptide effects in Figure 6 with those in Figure 5).

A very interesting biphasic, shrinkage–swelling response of RBC to the peptides BTM-P1 and BTM-P1d, observed in NaCl-sucrose medium (Figure 6), seems to reflect a time-dependent change in ion selectivity of the plasma membrane during formation of peptide pores, as suggested earlier [28]. In this respect, it is remarkable that the cell shrinkage phase coincided with electrical depolarization of the plasma membrane (Figure 6). These results can be explained assuming that the permeability of the plasma membrane to the internal chloride anions at the initial stage of peptide pore formation is significantly higher than that to the external sodium cations. These data reflect the particular properties of BTM-P1 and BTM-P1d, because the larger peptides BTM-P2 (Figure 6C) and BTM-P3 (Figure 6D) caused only monophasic cell response (swelling without preceding contraction).

As the peptide BTM-P1d was able to kill *A. aegypti* larvae at very low peptide concentrations (Figure 7), it might be related to its capacity to permeabilize mitochondrial and/or plasma membranes in the potential-dependent manner (Figure 5). The peptide BTM-P1 was almost ineffective in killing mosquito larvae (Figure 7), presumably due to its hydrolysis during the passage through the relatively long and highly proteolytic anterior midgut, which might prevent the appearance of significant peptide concentrations in the posterior midgut, where the apical membrane potential is more favourable for the potential-dependent insertion of the peptide into the membrane (Figure 9B).

A possible relationship between the proteolytic pathway length, influencing the concentration of active Cry toxin fragments, and the favourable membrane potential for the epithelium permeabilization is schematically shown in Figure 9B. According to this concept, the probability of permeabilization of the apical membrane is a product of the concentration of activated protoxin or of its active fragments in a given region of the lumen (Figure 9B, a) and of the value of favourable membrane potential (Figure 9B; curve b). It is consistent with the experimental data indicating that the most significant damage of *A. aegypti* larval epithelium under the action of Cry toxins is located in the posterior midgut, in comparison with the anterior midgut [68,69].

The observed increase with age in larval resistance to the toxic effect of BTM-P1d (Figure 7), non-sensitive to proteolysis, allows the assumption that possible changes in the electrical properties of the larval midgut might contribute to the known age-dependent larval susceptibility to the Cry toxins. This explanation is consistent with the recently published data that the over-expression of catalytical subunit β of mitochondrial F_1F_o ATP synthase induces hypersensitivity of *A. aegypti* larvae to the Cry11Aa toxin [70]. It might indicate that an increase in energy supply for transepithelial ion cycling increases corresponding membrane potentials and thus potential-dependent membrane permeabilization by the Cry toxins and by their shorter fragments. Similarly, permeabilization of mitochondrial membranes by BTM-P1 has been recently shown to strongly depend on the respiration rate and ATP synthase activity of mitochondria [28].

The precise mechanism of toxicity caused by *B. thuringiensis* Cry toxins in the midgut epithelial cells of insect larvae is not yet clear, although it has been established that it is due primarily to their ability to form pores in the plasma membrane of the midgut epithelial cells of susceptible insects [67]. It is widely accepted that the presence of specific receptors [9,10,12,13] is crucial for increasing the local concentrations of δ-endotoxins. Beyond the distribution of Cry toxin specific receptors, other factors might be involved in the pore-forming activity of toxins. It has been

© 2013 The Author(s) This is an Open Access article distributed under the terms of the Creative Commons Attribution Non-Commercial Licence (http://creativecommons.org/licenses/by-nc/2.5/) which permits unrestricted non-commercial use, distribution and reproduction in any medium, provided the original work is properly cited

shown for example that the membrane permeabilizing activity of Cry1Ac protoxin is significantly higher for the posterior than for the anterior regions of lepidopteran larvae; although no significant difference in the binding parameters for the protoxin were detected [71]. Moreover, the capability of permeabilization of artificial lipid membranes [11–21] and biomembranes [18,22,23] without specific receptors has been reported in the literature for some Cry-type toxins.

On the other hand, Cyt-type toxins are known to directly insert into the membrane and to form pores (see references in [72]). In addition, the binding of the Cyt1Aa protein to the brush border membrane of *A. aegypti* larvae enhanced the binding of Cry11Aa protoxin [6,72], synergistically increasing the toxic effect of Cry11A, as well as that of Cry4 toxins. This effect of Cyt1Aa, inserted into the membrane before Cry11Aa, has been explained by its possible functioning as a membrane-bound receptor for Cry11Aa [72].

The larval epithelial cell permeabilization by Cry toxins is explained by the widely accepted 'umbrella model' [4,5,73]. We have slightly modified this model converting it into the model of 'damaged umbrella' [27], which was based on a high membrane permeabilizing activity of the peptide BTM-P1 derived from the α2 helix segment of domain I of the Cry11Bb protoxin. According to 'damaged umbrella' model, the α2a helix or its part in the activated protoxin inserts into the membrane before or together with the hairpin domain composed of the α4–α5 helices. The membrane permeabilization by the polycationic peptide BTM-P1 [24,27,28], as well as by larger peptides BTM-P2 and BTM-P3 (Figure 6), strongly depends on membrane potential. It means that the insertion of the α2a helix should also be potential-dependent, and thus it might facilitate the insertion of the almost electrically neutral α4–α5 hairpin. The potential-dependent insertion of the α2a helix rib of the 'damaged umbrella' might be the initial stage of protoxin insertion into the membrane.

The results obtained in this work, the data published earlier [24,27,28] and the literature data related to the distribution of membrane potentials in the larval midgut (Figures 8 and 9), suggest a working hypothesis that the epithelial cells of the posterior midgut, in comparison with the anterior midgut, have the most favourable plasma membrane potential for the potential-dependent insertion of the α2a helix of the activated toxin into the apical membrane, thus facilitating the insertion of the α4–α5 hairpin. The electrical field distribution within the larval midgut, in addition to the distribution of the Cry-toxin-specific receptors, might be an important factor influencing the efficiency of membrane permeabilization by the Cry toxins and by their shorter fragments like the polycationic peptides studied in this work. This electrical factor seems to be crucial in determination of the larval midgut regions most susceptible to the Cry toxins.

AUTHOR CONTRIBUTION

Victor Lemeshko designed the study, conducted the experiments with mitochondria and RBCs, as well as developing the electrical model of toxicity of the Cry toxins. Sergio Orduz conducted the experiments with the mosquito larvae. Both authors contributed to writing the paper.

ACKNOWLEDGEMENT

We thank Gabriela Jaramillo Zapata for the technical assistance in experiments with mosquito larvae.

FUNDING

This study was supported by Colciencias (Colombia) [grant numbers 111852-12-8625, 362-2011].

REFERENCES

1 Höfte, H. and Whiteley, H. R. (1989) Insecticidal crystal proteins of *Bacillus thuringiensis*. Microbiol. Rev. **53**, 242–255
2 Schnepf, E., Crickmore, N., Van Rie, J., Lereclus, D., Baum, J., Feitelson, J., Zeigler, D. R. and Dean, D. H. (1998) *Bacillus thuringiensis* and its pesticidal crystal proteins. Microbiol. Mol. Biol. Rev. **62**, 775–806
3 Pigott, C. R. and Ellar, D. J. (2007) Role of receptors in *Bacillus thuringiensis* crystal toxin activity. Microbiol. Mol. Biol. Rev. **71**, 255–281
4 Gazit, E., Rocca, E., La, P., Sansom, M. S. and Shai, Y. (1998) The structure and organization within the membrane of the helices composing the pore-forming domain of *Bacillus thuringiensis* delta-endotoxin are consistent with an 'umbrella-like' structure of the pore. Proc. Natl. Acad. Sci. U.S.A. **95**, 12289–12294
5 Gerber, D. and Shai, Y. (2000) Insertion and organization within membranes of the delta-endotoxin pore-forming domain, helix 4-loop-helix 5, and inhibition of its activity by a mutant helix 4 peptide. J. Biol. Chem. **275**, 23602–23607
6 Bravo, A., Gill, S. S. and Soberón, M. (2007) Mode of action of *Bacillus thuringiensis* Cry and Cyt toxins and their potential for insect control. Toxicon **49**, 423–435
7 Lightwood, D. J., Ellar, D. J. and Jarrett, P. (2000) Role of proteolysis in determining potency of *Bacillus thuringiensis* Cry1Ac delta-endotoxin. Appl. Environ. Microbiol. **66**, 5174–5181
8 de Barros Moreira Beltrão, H. and Silva-Filha, M. H. (2007) Interaction of *Bacillus thuringiensis* svar. *israelensis* Cry toxins with binding sites from *Aedes aegypti* (Diptera: Culicidae) larvae midgut. FEMS Microbiol. Lett. **266**, 163–169
9 Hofmann, C., Vanderbruggen, H., Höfte, H., Van Rie, J., Jansens, S. and Van Mellaert, H. (1988) Specificity of *Bacillus thuringiensis* delta-endotoxins is correlated with the presence of high-affinity binding sites in the brush border membrane of target insect midguts. Proc. Natl. Acad. Sci. U.S.A. **85**, 7844–7848
10 Likitvivatanavong, S., Chen, J., Evans, A. M., Bravo, A., Soberon, M. and Gill, S. S. (2011) Multiple receptors as targets of Cry toxins in mosquitoes. J. Agric. Food Chem. **59**, 2829–2838
11 Gazit, E., Bach, D., Kerr, I. D., Sansom, M. S., Chejanovsky, N. and Shai, Y. (1994) The alpha-5 segment of *Bacillus thuringiensis* delta-endotoxin: *in vitro* activity, ion channel formation and molecular modelling. Biochem. J. **304**, 895–902
12 Schwartz, J. L., Lu, Y. J., Söhnlein, P., Brousseau, R., Laprade, R., Masson, L. and Adang, M. J. (1997) Ion channels formed in planar lipid bilayers by *Bacillus thuringiensis* toxins in the presence of *Manduca sexta* midgut receptors. FEBS Lett. **412**, 270–276

© 2013 The Author(s) This is an Open Access article distributed under the terms of the Creative Commons Attribution Non-Commercial Licence (http://creativecommons.org/licenses/by-nc/2.5/) which permits unrestricted non-commercial use, distribution and reproduction in any medium, provided the original work is properly cited

13 Peyronnet, O., Nieman, B., Généreux, F., Vachon, V., Laprade, R. and Schwartz, J. L. (2002) Estimation of the radius of the pores formed by the *Bacillus thuringiensis* Cry1C delta-endotoxin in planar lipid bilayers. Biochim. Biophys. Acta **567**, 113–122
14 Puntheeranurak, T., Uawithya, P., Potvin, L., Angsuthanasombat, C. and Schwartz, J. L (2004) Ion channels formed in planar lipid bilayers by the dipteran-specific Cry4B *Bacillus thuringiensis* toxin and its alpha1-alpha5 fragment. Mol. Membr. Biol. **21**, 67–74
15 Groulx, N., McGuire, H., Laprade, R., Schwartz, J. L. and Blunck, R. (2011) Single molecule fluorescence study of the *Bacillus thuringiensis* toxin Cry1Aa reveals tetramerization. J. Biol. Chem. **286**, 42274–42282
16 Rodríguez-Almazán, C., Reyes, E. Z., Zúñiga-Navarrete, F., Muñoz-Garay, C., Gómez, I., Evans, A. M., Likitvivatanavong, S., Bravo, A., Gill, S. S. and Soberón, M. (2012) Cadherin binding is not a limiting step for *Bacillus thuringiensis* subsp. *israelensis* Cry4Ba toxicity to *Aedes aegypti* larvae. Biochem. J. **443**, 711–717
17 Haider, M. Z. and Ellar, D. J. (1989) Mechanism of action of *Bacillus thuringiensis* insecticidal delta-endotoxin: interaction with phospholipid vesicles. Biochim. Biophys. Acta **978**, 216–222
18 Gazit, E. and Shai, Y. (1993) Structural and functional characterization of the alpha 5 segment of *Bacillus thuringiensis* delta-endotoxin. Biochemistry **32**, 3429–3436
19 Butko, P., Cournoyer, M., Pusztai-Carey, M. and Surewicz, W. K. (1994) Membrane interactions and surface hydrophobicity of *Bacillus thuringiensis* delta-endotoxin CrylC. FEBS Lett. **340**, 89–92
20 Masson, L., Schwab, G., Mazza, A., Brousseau, R., Potvin, L. and Schwartz, J. L. (2004) A novel *Bacillus thuringiensis* (PS149B1) containing a Cry34Ab1/Cry35Ab1 binary toxin specific for the western corn rootworm *Diabrotica virgifera virgifera* LeConte forms ion channels in lipid membranes. Biochemistry **43**, 12349–12357
21 Leetachewa, S., Katzenmeier, G. and Angsuthanasombat, C. (2006) Novel preparation and characterization of the alpha4-loop-alpha5 membrane-perturbing peptide from the *Bacillus thuringiensis* Cry4Ba delta-endotoxin. J. Biochem. Mol. Biol. **39**, 270–277
22 Drobniewski, F. A. and Ellar, D. J (1989) Purification and properties of a 28-kilodalton hemolytic and mosquitocidal protein toxin of *Bacillus thuringiensis* subsp. *darmstadiensis* 73-E10-2. J. Bacteriol. **171**, 3060–3067
23 Naimov, S., Boncheva, R., Karlova, R., Dukiandjiev, S., Minkov, I. and de Maagd, R. A. (2008) Solubilization, activation, and insecticidal activity of *Bacillus thuringiensis* serovar thompsoni HD542 crystal proteins. Appl. Environ. Microbiol. **74**, 7145–7151
24 Lemeshko, V. V., Arias, M. and Orduz, S. (2005) Mitochondria permeabilization by a novel polycation peptide BTM-P1. J. Biol. Chem. **280**, 15579–15586
25 Lemeshko, V. V., Guzman, F., Patarroyo, M. E., Segura, C. and Orduz, S. (2005) Synthetic peptide having an ionophoric and antimicrobial activity, U.S. Pat. 7,041,647.
26 Segura, C., Guzmán, F., Salazar, L. M., Patarroyo, M. E., Orduz, S. and Lemeshko, V. V. (2007) BTM-P1 polycationic peptide biological activity and 3D-dimensional structure, Biochem. Biophys. Res. Commun. **353**, 908–914
27 Arias, M., Orduz, S. and Lemeshko, V. V. (2009) Potential-dependent permeabilization of plasma membrane by the peptide BTM-P1 derived from the Cry11Bb1 protoxin, Biochim. Biophys. Acta **1788**, 532–537
28 Lemeshko, V. V. (2011) Permeabilization of mitochondria and red blood cells by polycationic peptides BTM-P1 and retro-BTM-P1. Peptides **32**, 2010–2020
29 Gutierrez, P., Alzate, O. and Orduz, S (2001) A theoretical model of the tridimensional structure of *Bacillus thuringiensis* subsp. *medellin* Cry 11Bb toxin deduced by homology modelling. Mem. Inst. Oswaldo Cruz **96**, 357–364
30 Clark, T. M., Koch, A. and Moffett, D. F. (1999) The anterior and posterior 'stomach' regions of larval *Aedes aegypti* midgut: regional specialization of ion transport and stimulation by 5-hydroxytryptamine. J. Exp. Biol. **202**, 247–252
31 Onken, H., Moffett, S. B. and Moffett, D. F. (2004) The transepithelial voltage of the isolated anterior stomach of mosquito larvae (*Aedes aegypti*): pharmacological characterization of the serotonin-stimulated cells. J. Exp. Biol. **207**, 1779–1787
32 Onken, H., Parks, S. K., Goss, G. G. and Moffett, D. F. (2009) Serotonin-induced high intracellular pH aids in alkali secretion in the anterior midgut of larval yellow fever mosquito *Aedes aegypti* L.J.. Exp. Biol. **212**, 2571–2578
33 Jagadeshwaran, U., Onken, H., Hardy, M., Moffett, S. B. and Moffett, D. F. (2010) Cellular mechanisms of acid secretion in the posterior midgut of the larval mosquito (*Aedes aegypti*). J. Exp. Biol. **213**, 295–300
34 Zhuang, Z., Linser, P. J. and Harvey, W. R (1999) Antibody to H(+) V-ATPase subunit E colocalizes with portasomes in alkaline larval midgut of a freshwater mosquito (*Aedes aegypti*). J. Exp. Biol. **202**, 2449–2460
35 Boudko, D. Y., Moroz, L. L., Linser, P. J., Trimarchi, J. R., Smith, P. J. and Harvey, W. R. (2001) *In situ* analysis of pH gradients in mosquito larvae using non-invasive, self-referencing, pH-sensitive microelectrodes. J. Exp. Biol. **204**, 691–699
36 Patrick, M. L., Aimanova, K., Sanders, H. R. and Gill, S. S. (2006) P-type Na+/K+-ATPase and V-type H+-ATPase expression patterns in the osmoregulatory organs of larval and adult mosquito *Aedes aegypti*. J. Exp. Biol. **209**, 4638–4651
37 Harvey, W. R., Boudko, D. Y., Rheault, M. R. and Okech, B. A. (2009) NHE(VNAT): an H+ V-ATPase electrically coupled to a Na+:nutrient amino acid transporter (NAT) forms an Na+/H+ exchanger (NHE). J. Exp. Biol. **212**, 347–357
38 Clark, T. M., Koch, A. and Moffett, D. F. (2000) The electrical properties of the anterior stomach of the larval mosquito (*Aedes aegypti*). J. Exp. Biol. **203**, 1093–1101
39 Wolfersberger, M. G (1992) V-ATPase-energized epithelia and biological insect control. J. Exp. Biol. **172**, 377–386
40 Harvey, W. R (2009) Voltage coupling of primary H+ V-ATPases to secondary Na+- or K+-dependent transporters. J. Exp. Biol. **212**, 1620–1629
41 Orduz, S., Realpe, M., Arango, R., Murillo, L. A. and Delécluse, A. (1998) Sequence of the Cry11Bb11 gene from *Bacillus thuringiensis* subsp. *medellin* and toxicity analysis of its encoded protein. Biochim. Biophys. Acta **1388**, 267–272
42 Restrepo, N., Gutierrez, D., Patiño, M. M., Thiéry, I., Delécluse, A. and Orduz, S (1997) Cloning, expression and toxicity of a mosquitocidal toxin gene of *Bacillus thuringiensis* subsp. *medellin*. Mem. Inst. Oswaldo Cruz **92**, 257–262
43 Bradford, M. M. (1976) A rapid and sensitive method for the quantitation of microgram quantities of protein utilizing the principle of protein-dye binding. Anal. Biochem. **72**, 248–254
44 Segura, C., Guzman, F., Patarroyo, M. E. and Orduz, S. (2000) Activation pattern and toxicity of the Cry11Bb1 toxin of *Bacillus thuringiensis* subsp. *medellin*. J. Invertebr. Pathol. **76**, 56–62
45 Lemeshko, V. V. and Kugler, W. (2007) Synergistic inhibition of mitochondrial respiration by anticancer agent erucylphospho-homocholine and cyclosporin A. J. Biol. Chem. **282**, 37303–37307
46 Raghuraman, H. and Chattopadhyay, A. (2005) Cholesterol inhibits the lytic activity of melittin in erythrocytes. Chem. Phys. Lipids **134**, 183–189
47 Wieckowski, M. R. and Wojtczak, L. (1998) Fatty acid-induced uncoupling of oxidative phosphorylation is partly due to opening of the mitochondrial permeability transition pore. FEBS Lett. **423**, 339–342

© 2013 The Author(s) This is an Open Access article distributed under the terms of the Creative Commons Attribution Non-Commercial Licence (http://creativecommons.org/licenses/by-nc/2.5/) which permits unrestricted non-commercial use, distribution and reproduction in any medium, provided the original work is properly cited

48 Lemeshko, V. V., Haridas, V., Quijano Perez, J. C. and Gutterman, J. U. (2006) Avicins, natural anticancer saponins, permeabilize mitochondrial membranes. Arch. Biochem. Biophys. **454**, 114–122
49 Lemeshko, V. V. (2002) Cytochrome *c* sorption-desorption effects on the external NADH oxidation by mitochondria: experimental and computational study. J. Biol. Chem. **277**, 17751–17757
50 Parker, J. C. and Castranova, V. (1984) Volume-responsive sodium and proton movements in dog red blood cells. J. Gen. Physiol. **84**, 379–401
51 Lemeshko, V. V. (2010) Membrane superficial charge modification affects mitochondrial permeabilization by derivatives of the polycationic peptide BTM-P1. Biophys. J., **98**, 278a
52 Clark, T. M., Hutchinson, M. J., Huegel, K. L., Moffett, S. B. and Moffett, D. F. (2005) Additional morphological and physiological heterogeneity within the midgut of larval *Aedes aegypti* (Diptera: Culicidae) revealed by histology, electrophysiology, and effects of *Bacillus thuringiensis* endotoxin. Tissue Cell **37**, 457–468
53 Moffett, D. F., Jagadeshwaran, U., Wang, Z., Davis, H. M., Onken, H. and Goss, G. G. (2012) Signaling by intracellular Ca2+ and H+ in larval mosquito (*Aedes aegypti*) midgut epithelium in response to serosal serotonin and lumen pH. J. Insect Physiol. **58**, 506–512
54 Okech, B. A., Boudko, D. Y., Linser, P. J. and Harvey, W. R. (2008) Cationic pathway of pH regulation in larvae of *Anopheles gambiae*. J. Exp. Biol. **211**, 957–968
55 Okech, B. A., Meleshkevitch, E. A., Miller, M. M., Popova, L. B., Harvey, W. R. and Boudko, D. Y. (2008) Synergy and specificity of two Na+-aromatic amino acid symporters in the model alimentary canal of mosquito larvae. J. Exp. Biol. **211**, 1594–1602
56 Onken, H. and Moffett, D. F. (2009) Revisiting the cellular mechanisms of strong luminal alkalinization in the anterior midgut of larval mosquitoes. J. Exp. Biol. **212**, 373–377
57 Azuma, M., Harvey, W. R. and Wieczorek, H. (1995) Stoichiometry of K+/H+ antiport helps to explain extracellular pH 11 in a model epithelium. FEBS Lett. **361**, 153–156
58 Pullikuth, A. K., Aimanova, K., Kang'ethe, W., Sanders, H. R. and Gill, S. S. (2006) Molecular characterization of sodium/proton exchanger 3 (NHE3) from the yellow fever vector, *Aedes aegypti*. J. Exp. Biol. **209**, 3529–3544
59 Sterling, K. M., Okech, B. A., Xiang, M. A., Linser, P. J., Price, D. A., Vanekeris, L., Becnel, J. J. and Harvey, W. R (2012) High affinity (3)H-phenylalanine uptake by brush border membrane vesicles from whole larvae of *Aedes aegypti* (AaBBMVw). J. Insect Physiol. **58**, 580–589
60 Boudko, D. Y (2012) Molecular basis of essential amino acid transport from studies of insect nutrient amino acid transporters of the SLC6 family (NAT-SLC6). J. Insect Physiol. **58**, 433–449
61 Harvey, W. R., Okech, B. A., Linser, P. J., Becnel, J. J., Ahearn, G. A. and Sterling, K. M. (2010) H^+ V-ATPase-energized transporters in brush border membrane vesicles from whole larvae of *Aedes aegypti*. J. Insect Physiol. **56**, 1377–1389
62 Linser, P. J., Smith, K. E., Seron, T. J. and Neira Oviedo, M. (2009) Carbonic anhydrases and anion transport in mosquito midgut pH regulation. J. Exp. Biol. **212**, 1662–1671
63 Rajasekaran, S. A., Beyenbach, K. W. and Rajasekaran, A. K. (2008) Interactions of tight junctions with membrane channels and transporters. Biochim. Biophys. Acta **1778**, 757–769
64 Beyenbach, K. W. and Piermarini, P. M. (2011) Transcellular and paracellular pathways of transepithelial fluid secretion in Malpighian (renal) tubules of the yellow fever mosquito *Aedes aegypti*. Acta Physiol. **202**, 387–407
65 Lemeshko, V. V. (2010) Potential-dependent membrane permeabilization and mitochondrial aggregation caused by anticancer polyarginine-KLA peptides. Arch. Biochem. Biophys. **493**, 213–220
66 Tanaka, S., Yoshizawa, Y. and Sato, R. (2012) Response of midgut epithelial cells to Cry1Aa is toxin-dependent and depends on the interplay between toxic action and the host apoptotic response. FEBS J. **279**, 1071–1079
67 Vachon, V., Laprade, R. and Schwartz, J. L. (2012) Current models of the mode of action of *Bacillus thuringiensis* insecticidal crystal proteins: a critical review. J. Invertebr. Pathol. **111**, 1–12
68 Charles, J. F (1987) Ultrastructural midgut events in Culicidae larvae fed with *Bacillus sphaericus* 2297 spore/crystal complex. Ann. Inst. Pasteur Microbiol. **138**, 471–484
69 de Melo, J. V., Vasconcelos, R. H., Furtado, A. F., Peixoto, C. A. and Silva-Filha, M. H. (2008) Ultrastructural analysis of midgut cells from *Culex quinquefasciatus* (Diptera: Culicidae) larvae resistant to *Bacillus sphaericus*. Micron **39**, 1342–1350
70 Cancino-Rodezno, A., Lozano, L., Oppert, C., Castro, J. I., Lanz-Mendoza, H., Encarnación, S., Evans, A. E., Gill, S. S., Soberón, M., Jurat-Fuentes, J. L. and Bravo, A (2012) Comparative proteomic analysis of *Aedes aegypti* larval midgut after intoxication with Cry11Aa toxin from *Bacillus thuringiensis*. PLoS ONE **7**, e37034
71 Rodrigo-Simón, A., Caccia, S. and Ferré, J. (2008) *Bacillus thuringiensis* Cry1Ac toxin-binding and pore-forming activity in brush border membrane vesicles prepared from anterior and posterior midgut regions of lepidopteran larvae. Appl. Environ. Microbiol. **74**, 1710–1716
72 Pérez, C., Fernandez, L. E., Sun, J., Folch, J. L., Gill, S. S., Soberón, M. and Bravo, A. (2005) *Bacillus thuringiensis* subsp. *israelensis* Cyt1Aa synergizes Cry11Aa toxin by functioning as a membrane-bound receptor. Proc. Natl. Acad. Sci. U.S.A. **102**, 18303–18308
73 Li, J., Carroll, J. and Ellar, D. J. (1991) Crystal structure of insecticidal delta-endotoxin from *Bacillus thuringiensis* at 2.5 Å resolution. Nature **353**, 815–821

Received 10 October 2012; accepted 19 October 2012

Published as Immediate Publication 19 October 2012, doi 10.1042/BSR20120101

© 2013 The Author(s) This is an Open Access article distributed under the terms of the Creative Commons Attribution Non-Commercial Licence (http://creativecommons.org/licenses/by-nc/2.5/) which permits unrestricted non-commercial use, distribution and reproduction in any medium, provided the original work is properly cited